Clays and Clay Minerals, Vol. 44, No. 6, 825–834, 1996.

EXPERIMENTAL TRANSFORMATION OF KAOLINITE TO HALLOYSITE

BALBIR SINGH AND IAN D. R. MACKINNON

Centre for Microscopy and Microanalysis, The University of Queensland, Brisbane, Qld 4072, Australia

Abstract—A well-characterized kaolinite has been hydrated in order to test the hypothesis that platey kaolinite will roll upon hydration. Kaolinite hydrates are prepared by repeated intercalation of kaolinite with potassium acetate and subsequent washing with water. On hydration, kaolinite plates roll along the major crystallographic directions to form tubes identical to proper tubular halloysite. Most tubes are elongated along the *b* crystallographic axis, while some are elongated along the *a* axis. Overall, the tubes exhibit a range of crystallinity. Well-ordered examples show a 2-layer structure, while poorly ordered tubes show little or no 3-dimensional order. Cross-sectional views of the formed tubes show both smoothly curved layers and planar faces. These characteristics of the experimentally formed tubes are shared by natural halloysites. Therefore, it is proposed that planar kaolinite can transform to tubular halloysite.

Key Words—Halloysite, Hydration, Intercalation, Kaolinite, Rolling, Tetrahedral Rotation.

INTRODUCTION

It is well-accepted that halloysite rolls due to lateral misfit of the smaller octahedral and larger tetrahedral sheet (Bates et al. 1950; Bailey 1989). However, it is still not clear why tetrahedral rotation, a mechanism evident in kaolinite and many 2:1 minerals to reduce the dimensions of the tetrahedral sheet (Radoslovich 1963), does not take place in halloysite (Giese 1988). Bailey (1989) proposed that tetrahedral rotation in halloysites is blocked by water molecules and hydrated exchangeable cations seated in the hexagonal cavity of the basal oxygen plane. Therefore, halloysite layers roll in order to accommodate the lateral misfit. Bailey's model implies that tetrahedral rotation is the preferred mechanism and that the rolling mechanism comes into effect only when tetrahedral rotation is restricted. According to this model, all tubular and spheroidal halloysites crystallize in their current rolled form and a planar kaolin 1:1 layer cannot roll after crystallization.

Singh (1996) presented a theoretical comparison of forces in the tetrahedral sheet that oppose tetrahedral rotation and rolling. That paper showed that, in the absence of strong interlayer hydrogen bonding, rolling encounters considerably less opposition in comparison to tetrahedral rotation to correct the same amount of misfit. Thus, rolling is the preferred mechanism for hydrated halloysite to accommodate the misfit, and does not require tetrahedral rotation to be blocked as Bailey (1989) proposed. Singh (1996) also suggested that the kaolin structure may effect a switch from one mechanism to the other, depending on the state of hydration and the resultant strength of hydrogen bonding. If the model by Singh (1996) is valid, a planar kaolinite layer will roll once interlayer hydrogen bonding is weakened by hydration and expansion of the interlayer space. This paper reports rolling of a well-characterized platey kaolinite after a series of hydration experiments.

The terminology and criteria used to distinguish halloysite from kaolinite are inconsistent. In this study, the term "kaolin" is used to refer to kaolinite and halloysite, collectively. Crystals with a platey morphology and kaolin chemical composition are considered to be kaolinite, and those with a cylindrical morphology and the same composition, halloysite.

MATERIALS AND METHODS

Several procedures can be used to prepare hydrates of kaolin group minerals. Wada (1965) successfully prepared 14-Å intercalates of halloysite, kaolinite and nacrite by dry-grinding with potassium acetate (KAc). Hydrates of these minerals were formed by subsequent washing of the intercalate with water to remove the salt. Costanzo et al. (1980) prepared a 10-Å hydrate of kaolinite using dimethylsulfoxide (DMSO) and ammonium fluoride. Similarly, hydrazine, formamide and N-methyl formamide have been used with varying success to prepare hydrates of kaolinite (Costanzo et al. 1984). This study employs intercalation with KAc and subsequent washing due to simplicity of experimentation and the known capacity of KAc to cause expansion of kaolinite up to 14 Å.

Several kaolinites described by Uwins et al. (1993) have been initially tested in this study. Georgia kaolinite (KGa-1, available from the Source Clay Mineral Repository of The Clay Minerals Society) was selected for detailed investigations because it intercalates very well and consists mainly of euhedral platey crystals with no halloysite tubes or other rolled particles. Georgia kaolinite has also been studied in similar intercalation experiments by other workers (Costanzo and Giese 1985; Uwins et al. 1993; Wada 1961).

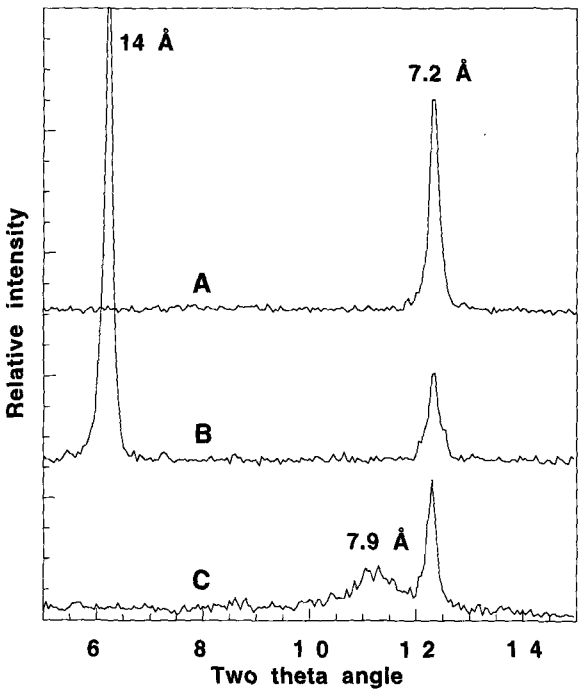

Figure 1. XRD pattern of (A) Georgia kaolinite, (B) its intercalation complex with KAc and (C) washed intercalation complex. An intermediate reflection at 7.9 Å appears after washing the intercalation complex with water.

About 3 g of kaolinite are thoroughly mixed with 25 ml of saturated solution of KAc in centrifuge tubes and allowed to intercalate for 2 d at 80 °C. The progress of intercalation is monitored by periodic X-ray diffraction (XRD) of the intercalates. After maximum intercalation has occurred, based upon a maximum ratio of 14 to 7 Å peak intensity, the suspensions are centrifuged, and supernatant KAc solution is removed. Next, the samples are washed with deionized water to remove KAc from the interlayer. The intercalation and washing process is repeated several times while periodically examining XRD traces before and after washing. After few initial cycles of intercalation and washing, a contact time of approximately 15 min with KAc is sufficient to effect maximum intercalation. Neither grinding, ultrasonification nor any other treatment involving severe external force is used in the procedure in order to preserve the morphological data on transformations caused by intrinsic structural forces after hydration.

Oriented samples of intercalated and washed materials for XRD are prepared by sedimentation of undiluted suspensions on ceramic plates under gentle suction. The washed samples are scanned while moist and after appropriate drying conditions. The oriented samples are scanned rapidly (2°/min) in order to avoid drying during scanning. Randomly oriented samples of the dry powdered materials are prepared by standard methods. All samples are analyzed using a Siemens D5000 diffractometer with graphite monochromator and Cu$K\alpha$ radiation. Particle size distributions are measured by laser scattering in a flow-through cell using a Malvern Mastersizer E instrument and methodology described by Mackinnon et al. (1993).

Samples for transmission electron microscopy (TEM) are prepared in 2 ways. Small droplets of very dilute suspensions are dried on carbon-coated Cu grids. Other samples are prepared by microtomy. Dilute suspensions are settled in a tube using a centrifuge to obtain a thick mass of oriented sample. The settled samples are dried and then vacuum-impregnated with Spurr's resin. Ultrathin sections are cut normal to the base of the impregnated sample with a diamond knife using a Reichert-Jung microtome. All TEM samples were investigated using a JEOL 4000FX electron microscope operated at 400 kV.

RESULTS AND DISCUSSION

Bulk Properties of Intercalates and Hydrates

The Georgia kaolinite intercalated readily with a saturated solution of KAc (Figure 1). More than 80% intercalation, indicated by a reduction in the intensity of the 7.2-Å reflection and appearance of a reflection at 14 Å, was achieved in about 2 d. Rigorous methods of intercalation, such as grinding of salt with clay (Wada 1961; Uwins et al. 1993) were avoided, as these procedures may severely deform the structure and morphology of kaolinite.

The penetration of KAc molecules into the layers expanded the *c* axis from 7.2 to 14 Å (Figure 1). The intercalation complex collapsed to 11.4 Å (not shown) upon heating at 105 °C and restored to 14 Å after exposure to humid air over a period of few d. The collapse of the intercalate basal spacing to 11.4 Å upon heating and its subsequent restoration in humid air indicate the presence of water in the interlayer space along with KAc. On the basis of size of K^+ cation and van der Waals radii of CH_3 and H_2O molecules, Wada (1961) suggested that the K^+ fits in the hexagonal cavity of the basal oxygen plane and the remaining space in the interlayer is occupied by CH_3COO and a monolayer of water. Upon washing of the intercalate with water, the 14-Å basal spacing disappeared and, in addition to an increase in the intensity of the 7.2-Å reflection, a broad reflection at ~7.9 Å (hereinafter referred to as the intermediate reflection) appeared (Figure 1).

The position of the intermediate reflection depends on the duration and degree of intercalation. For short periods of initial intercalation (that is, a few h), the position varied between 7.3 and 7.5 Å, which is consistent with the work of Wada (1961) and Deed et al. (1966). The higher-order reflections of the intermediate reflection showed non-integral spacings, which

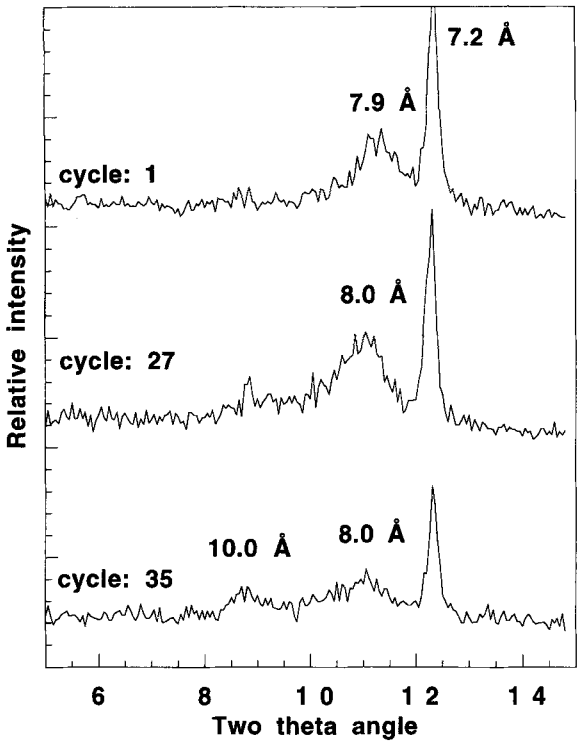

Figure 2. XRD patterns of Georgia kaolinite after a number of intercalation and washing cycles. The intermediate reflection broadens with increasing number of intercalation and washing cycles, and after 35 cycles a broad reflection at 10 Å appears.

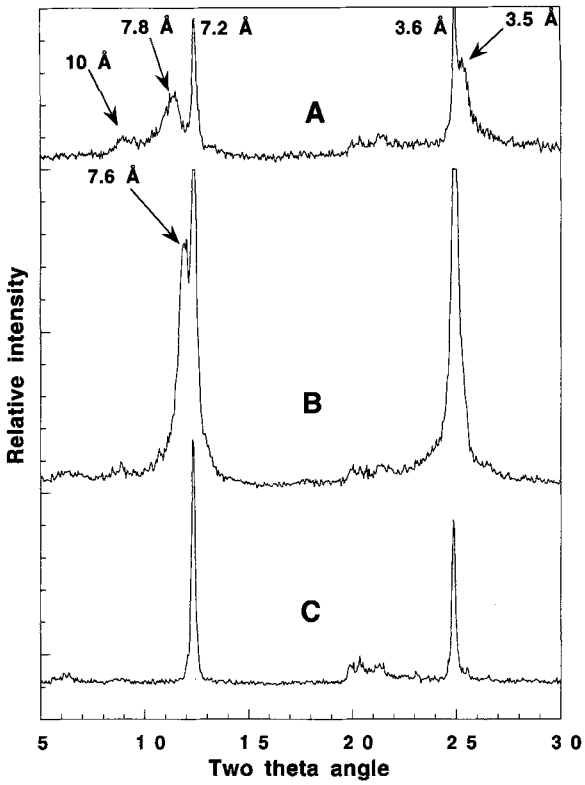

Figure 3. XRD pattern of the wet kaolinite hydrate (A) and after air-drying it (B, C). The intermediate reflection gradually shifted to the higher angle (B) and eventually merged with the 7.2-Å reflection after air-drying for 3 d (C).

suggests that it represents interstratification rather than unit-cell periodicities. Wada (1965) considered that the intermediate reflection is due to interstratification of 7.2-Å and 10-Å spacing of the hydrated layers. Similar intermediate reflections were also observed by Churchman et al. (1972) and Kohyama et al. (1978) during dehydration of a hydrated halloysite. In agreement with Wada (1965), these authors also considered that only 10-Å and 7.2-Å layers exist in partially dehydrated halloysite, and that the observed intermediate reflections are due to interstratification of domains of hydrated (10-Å) and dehydrated (7.2-Å) layers. However, Costanzo and Giese (1985) showed that a third phase with a basal spacing of 8.6 Å may also occur, and they argued that the 7.9-Å spacing may also be the result of interstratification of 7.2-Å and 8.6-Å layers.

Hydration is always accompanied by considerable disordering of the kaolinite structure (Wada 1961; Costanzo et al. 1984), leading to the paradigm that the creation of disorder is a necessary and integral part of the hydration of kaolinite (Costanzo et al. 1984). The conventional model holds that layers slip in the *a, b* or both (random) directions when they collapse upon washing of the intercalate, resulting in layer stacking disorder. On the basis of this assumption, it seems likely that repeated intercalation and washing would produce widespread stacking disorder and, thus, would increase the proportion of hydrated layers.

XRD patterns of the hydrates after repeated intercalation and washing are shown in Figure 2. With an increasing number of intercalation and washing cycles, the intermediate reflection broadens and moves to a lower 2θ angle. After 35 intercalation and washing cycles, a broad reflection at 10 Å appears. However, the residual 7.2-Å reflection still remains after 35 intercalation and washing cycles, suggesting that some kaolinite particles are not affected by this treatment.

The 10-Å reflection disappears after air drying overnight and the intermediate reflection gradually sharpens and moves toward the 7.2-Å reflection (Figure 3). After air drying for 3 d, the intermediate reflection eventually merges with the 7.2-Å reflection. The intermediate reflection exhibits non-integral second-order reflections during the drying cycle. This observation is consistent with the interpretation that the intermediate reflection is due to random interstratification of 10-Å and 7.2-Å layers within partially hydrated particles.

https://doi.org/10.1346/CCMN.1996.0440614 Published online by Cambridge University Press

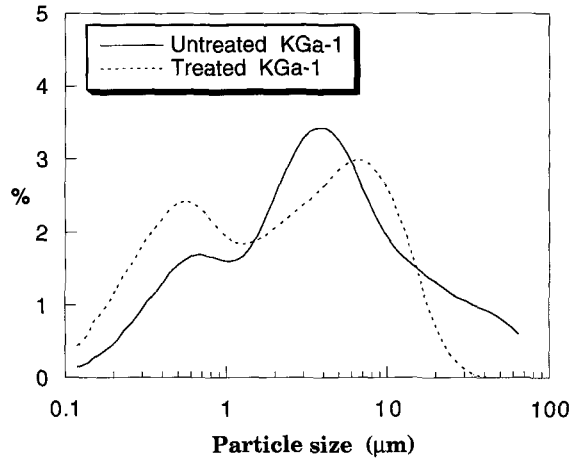

Figure 4. Particle size distribution of Georgia kaolinite before and after repeated intercalation and washing treatment.

After about 35 cycles, a clear difference in the properties of the hydrate compared with untreated kaolinite is noticed. The suspensions become considerably voluminous and viscous, and readily flocculate with a comparatively stable suspension at pH 10. The surface area and cation exchange capacity (CEC) for the treated sample increase significantly in comparison with the untreated Georgia kaolinite. The surface area and CEC for treated samples are ~10 m^2 g^{-1}, 32 meq/100 g, respectively, whereas the corresponding values for Georgia kaolinite are 6 m^2 g^{-1} and 10 meq/100 g, respectively. The particle size distribution of the treated sample and Georgia kaolinite are shown in Figure 4. The treated sample has a higher proportion of the fine-grained fraction (<1 μm) and lower proportion of coarse particles (>15 μm) in comparison with the untreated Georgia kaolinite. It appears that larger particles have exfoliated or fragmented to produce smaller particles as a result of repeated intercalation and washing.

Morphology

A typical TEM micrograph of Georgia kaolinite is presented in Figure 5. It shows that Georgia kaolinite consists of euhedral platey crystals with no halloysite tubes or laths. Therefore, any rolled forms present in a hydrated derivative of Georgia kaolinite may be considered a transformation product of platey crystals.

A low magnification TEM micrograph of Georgia kaolinite after 35 cycles of KAc intercalation and washing is shown in Figure 6. Most of the material exhibits longitudinal morphologies (indicated by arrowheads), either attached to platey crystals or existing as discrete particles. Selected area electron diffraction (SAED) and high resolution images show that these longitudinal features represent rolled or folded layers of previously platey crystals. The mottled contrast for some of these features is due to diffraction by the (001) plane(s) of the tube walls parallel to the electron beam. Several isolated tubes similar to proper halloysite tubes (Singh and Gilkes 1992) as well as perfectly platey euhedral kaolinite crystals are present.

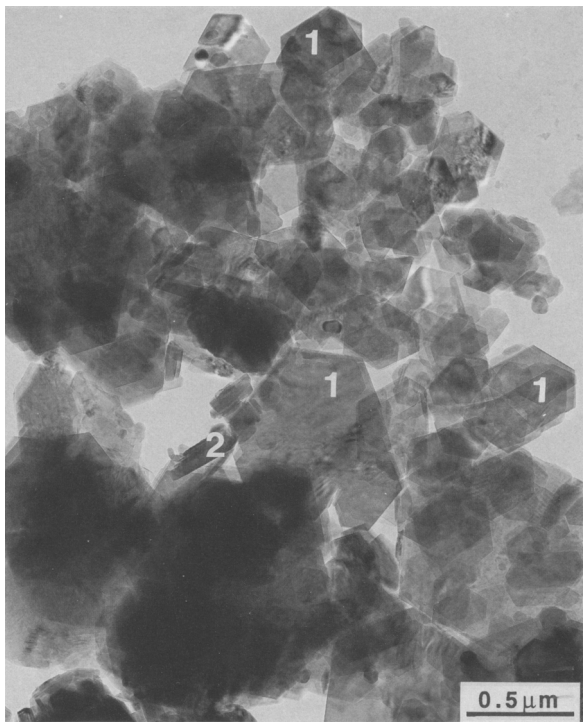

Figure 5. TEM of Georgia kaolinite showing euhedral kaolinite crystals (1) with no halloysite tubes or laths. The occasional longitudinal particles (2) seen in the micrograph are small platey kaolinite crystals with their (001) face parallel to the electron beam.

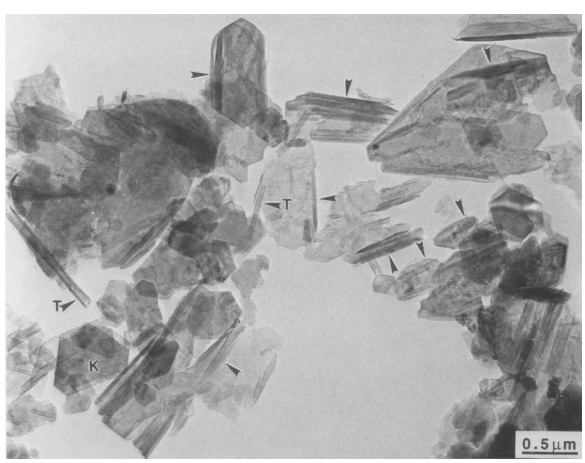

Figure 6. TEM of Georgia kaolinite after more than 35 KAc intercalation and washing cycles. The abundant longitudinal features (indicated by arrowheads) attached to the plates represent the rolled/folded kaolinite layers. Some tubes (T) similar to natural halloysite tubes and some perfectly platey kaolinite crystals are also present.

https://doi.org/10.1346/CCMN.1996.0440614 Published online by Cambridge University Press

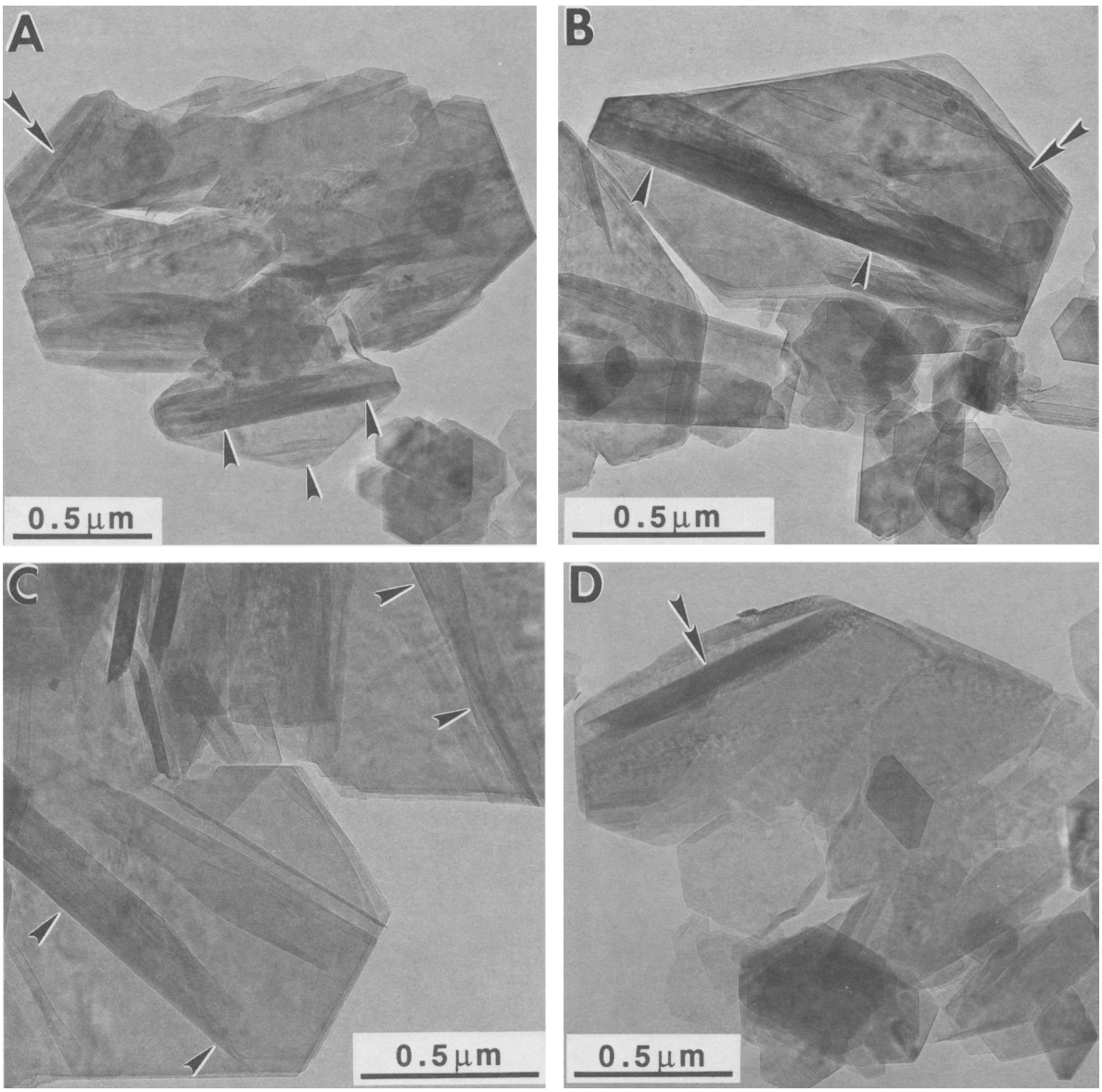

Figure 7. High magnification TEMs of kaolinite hydrate showing orientation of tubes with the parent kaolinite crystals. The tubes are either normal (single arrowheads in A, B and C) or parallel (double arrowheads in A, B and D) to a major crystallographic factor of the platey crystal, demonstrating that direction of rolling is controlled by crystallographic direction in the kaolinite structure.

The rolling direction of the tubes appears to be controlled by the crystallography of the parent kaolinite plates. The long axis of the tubes is always either normal or parallel to a major face of the kaolinite crystal. This relationship between the parent material and the derived tubes is apparent because Georgia kaolinite has well-defined crystal faces. For example, in Figure 7, tubes denoted by single arrows show a long axis normal to a crystal face, while those denoted by double arrows show long axes parallel to the crystal face. These 2 rolling orientations are sometimes present on a single large kaolinite plate (Figures 7a and 7b). The schematic diagrams in Figure 8 illustrate the observed rolling modes of kaolinite plates to form tubes after many intercalation and washing cycles.

The formed tubes are uniform in diameter along the length of the tube. This observation implies that a cylindrical rather than a cone-shaped structure is formed. A plate rolled to form cones has a random axis of rolling. Thus, the absence of cones is consistent with the observation that the rolling axis is always either parallel or normal to one of the major crystallographic directions. The thickness of the tube walls, determined by the width of coherently diffracting regions showing

https://doi.org/10.1346/CCMN.1996.0440614 Published online by Cambridge University Press

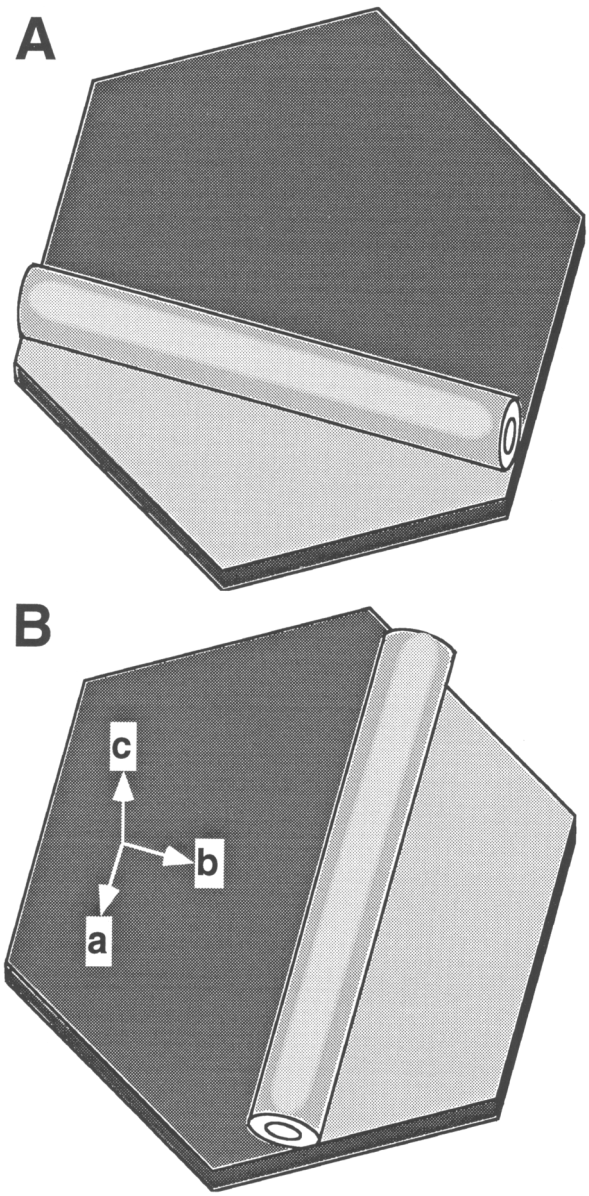

Figure 8. A schematic diagram illustrating the observed spatial relationship of the tubes with platey crystals. The observed tubes are either normal (A) or parallel (B) to a major crystallographic face of the platey crystals.

mottled contrast, varies from 10 to 50 nm. This dimension is similar to tube-wall thicknesses measured for natural halloysites (Singh and Gilkes 1992).

The morphological data (Figure 9) provided by the ultrathin section cut normal to the basal plane of the plates are consistent with the above interpretation. The kaolinite plates exfoliate and roll to form tubes with a central hole. The cross-sections of tubes show smoothly curved layers as well as planar faces. The planar faces are commonly observed in natural halloysite (Dixon and McKee 1974; Singh and Gilkes 1992), and are considered to be due to flattening caused by dehydration.

Electron Diffraction

SAED patterns of the individual tubes occur in 2 primary forms. A typical example of the first type is shown in Figure 10. This diffraction pattern is characteristic of a tubular crystal showing streaks parallel to the a^* axis. The a^* and c^* axes are on a common axis perpendicular to the b^* axis. Thus, the axis of rotation of the tube (tube axis) is parallel to the b crystallographic axis of the parent kaolinite plate. The pattern shows considerable 3-dimensional order. The distance between the first (02l) reflection and the (020) reflection is ~14 Å, which is double the spacing of the first basal reflection. Therefore, on the basis of a 2-layer periodicity (Honjo et al. 1954; Kohyama et al. 1978), the first basal reflection is indexed as (002) and first (02l) reflection as (021). In this pattern, the (11l) reflections are also well-resolved, demonstrating that the tubular crystal has high crystallinity. A similar SAED pattern for a natural halloysite with well-resolved (11l) and (02l) reflections was observed by Honjo et al. (1954). Other poorly-ordered examples of this type of SAED pattern with poorly resolved (02l) and (11l) reflections also occurred in these modified kaolinites.

A typical example of the second type of SAED pattern is shown in Figure 11. In this pattern, the c^* axis and the direction of streaking is parallel to the b^* axis, demonstrating that the tube axis is parallel to the a crystallographic axis. These types of diffraction patterns are less common than the example given above. Well-ordered diffraction patterns showing well-resolved (11l) and (20l) reflections are not present. Interestingly, natural halloysites with the tube axis parallel to the a axis do occur, but are similarly uncommon. For example, Honjo et al. (1954) found some tubes in the Hong Kong kaolin sample elongated along the a axis, while most tubes in the same sample were elongated along the b axis.

The observed types of electron diffraction patterns from these tubes are consistent with the occurrence of 2 modes of rolling of platey crystals to form tubes (Figure 8). Tubes characterized by the first type of SAED patterns (Figure 10) form from platey crystals with the axis of rotation normal to a major face of a platey kaolinite crystal (Figure 8a). Tubes characterized by the second type of SAED pattern (Figure 11) form from platey crystals with the axis of rotation parallel to a major face of a kaolinite crystal (Figure 8b).

GENERAL DISCUSSION AND CONCLUSIONS

Costanzo et al. (1980) prepared kaolinite hydrate by intercalation with DMSO and subsequent ammonium fluoride treatment before washing. DMSO intercalation expands the kaolinite layers to 11 Å and, unless

https://doi.org/10.1346/CCMN.1996.0440614 Published online by Cambridge University Press

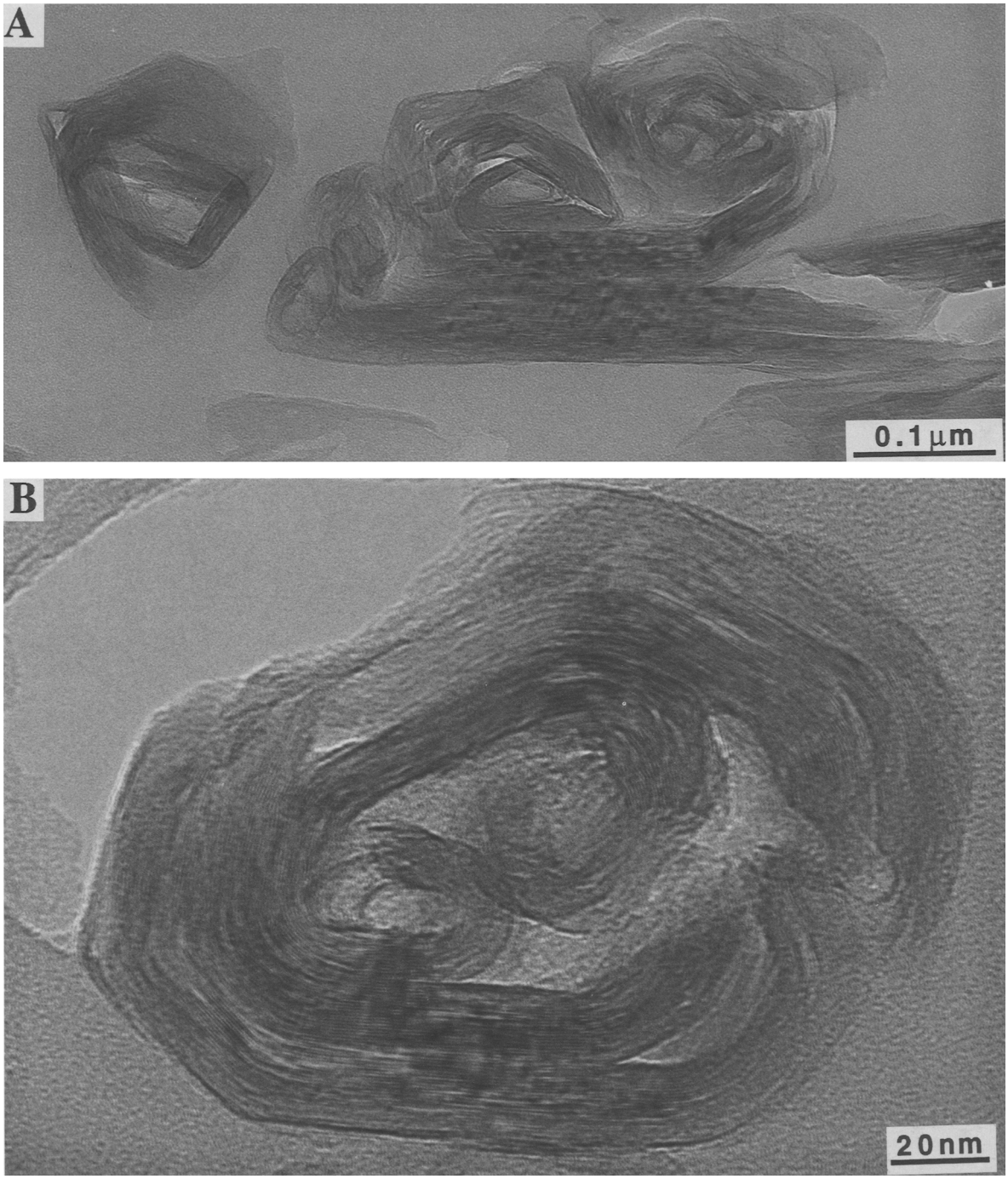

Figure 9. A) TEM of an ultrathin cross-section of plate exfoliated and rolled to form tubes. B) Cross-section of a formed tube showing smoothly curved layers and planar faces of the tube.

subsequently treated with NH_4F to replace the OH groups with F, the basal spacings return to 7.2 Å upon washing the intercalate. On the basis of heat capacities of several kaolinites and their intercalates prepared using a number of intercalates, Costanzo et al. (1984) found that hydration is positively co-related to the degree of stacking disorder created by a given intercalation process. The substitution of OH by F contributes indirectly to hydration by weakening the interlayer bonding, since there is no attraction between the O and F atoms (Wolfe and Giese 1978). In the present study, KAc intercalation produces a hydrate of kaolinite

https://doi.org/10.1346/CCMN.1996.0440614 Published online by Cambridge University Press

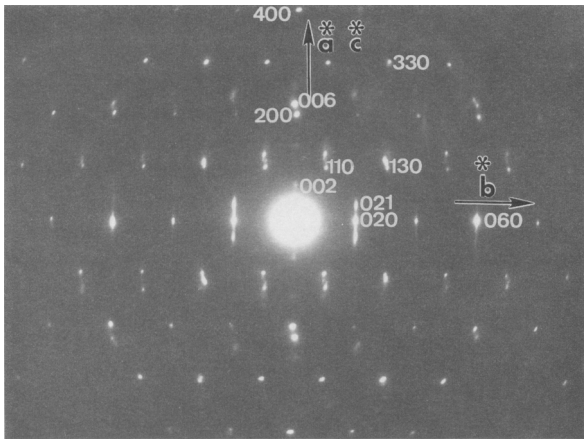

Figure 10. A typical example of one type of SAED pattern of tubes. The pattern is indexed on the basis of a 2-layer (c = 14 Å) structure, and demonstrates that axis of rotation is along the direction of the b axis. The pattern is identical to a typical SAED pattern of halloysite tube.

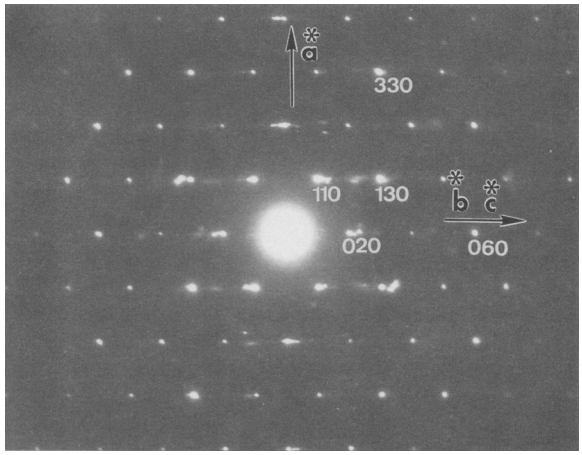

Figure 11. A typical example of the second type of SAED patterns of tubes. The axis rotation in this type is parallel to the a crystallographic axis of the kaolinite crystal.

without replacement of OH with F, probably because KAc is able to expand the kaolinite layers up to 14 Å. This greater expansion in comparison to DMSO intercalation (only to 11 Å) creates greater stacking disorder and further weakening of interlayer bonding. Each additional cycle of intercalation and washing progressively extends the level of stacking disorder and hydration within a specific sample. Thus, the underlying cause of hydration in this study and in the work by Costanzo et al. (1980, 1984) is probably the same.

Rolling of the kaolinite plates is noticeable only after 10 intercalation and washing cycles. However, after 30 cycles, the effect is extensive, present in many crystals and clearly visible in TEM and SEM images. Apparently, repeated expansion and contraction of the hydrated layers is necessary for rolling to occur.

In general, the morphology of the rolled form is identical to natural tubular halloysites. The diameter and length of tubes vary considerably, as is commonly observed for natural halloysites. Presumably, these tube characteristics are controlled by the uniformity of hydration, thickness, lateral size and crystallinity of the parent kaolinite plates. All of these properties usually show some variation within a single specimen of most kaolinites, including Georgia kaolinite (Uwins et al. 1993), so that variation in the morphology of the rolled form is expected.

The rolled particles obtained from the repeated intercalation of kaolinite showed SAED patterns identical to those obtained for natural halloysites (Honjo et al. 1954; Singh and Gilkes 1992). The most crystalline tubes exhibit 2-layer periodicity, which is a common characteristic of natural halloysites. The tube axis is either parallel to the b or the a crystallographic axis, but predominantly parallel to the b axis of the parent kaolinite structure. This relationship is also remarkably consistent with natural halloysites, which are primarily elongated along the b crystallographic axis. Detailed drying and intercalation characteristics of the kaolinite hydrate have not been investigated in the present study. However, Costanzo et al. (1980) and Costanzo and Giese (1985) have shown that these properties of kaolinite hydrates are similar to those of natural halloysites. Thus, the Georgia kaolinite has clearly rolled after successive intercalation and washing cycles to produce tubes that are indistinguishable from natural halloysite tubes with respect to their morphology, structure, chemical composition, drying and intercalation characteristics.

Recent TEM investigations of natural samples have also indicated that platey kaolinite may roll or curve to produce halloysite tubes (Robertson and Eggleton 1991; Singh and Gilkes 1992). In the kaolin material described by Singh and Gilkes (1992), kaolinite plates fractured and rolled to form an array of oriented halloysite tubes. Similarly, Robertson and Eggleton (1991) observed that kaolinite plates formed by weathering of muscovite fanned (exfoliated at the edges) and folded to form tubes. However, the reasons for hydration of kaolinite in a natural environment are not clear.

A Mechanism for Rolled Layers

Thin edges of clay minerals, including kaolinite, have been observed to curl in the electron microscope. Bailey (1989) attributes this phenomenon to the influence of surface tension. The thickness of rolled plates observed in this study varies between 10 and 50 nm. Therefore, rolling of the plates observed in this study cannot be attributed to surface tension. Furthermore, surface tension is likely to cause curling of sheets in a random direction, contrary to the observations of this study. In these samples, the tube axis is always parallel

to major crystallographic directions, indicating that rolling occurred in response to a dynamic balance of intrinsic crystallographic or structural forces rather than in response to a randomly generated external force. The vacuum in electron microscopes is known to cause flattening of halloysite tubes (Kohyama et al. 1978). Thus, the observed curvature of these particles may be an underestimate of the actual curvature in the hydrated state.

In dioctahedral clays, the lateral dimensions of the Si-tetrahedral sheet (b = 9.164 Å) are significantly larger than that of the Al-octahedral sheet (b = 8.665 Å). The misfit of the sheets can be corrected either by tetrahedral rotation (as in the case of kaolinite) or by rolling. Since the publication of a tetrahedral rotation model by Radoslovich (1963), it has been unclear why halloysite prefers to form tubes while misfit can be readily corrected by tetrahedral rotation (Giese 1988; Bailey 1989). Various authors have attempted to explain this discrepancy, and a companion paper (Singh 1996) outlines the development of thinking on this topic. For example, Bailey (1989) suggested that tetrahedral rotation in halloysite is blocked by water and exchangeable cations seated in the hexagonal cavity of the tetrahedral sheet. According to this model, all tubular and spheroidal halloysites crystallize in their current rolled form, which is clearly not consistent with the experimental evidence obtained in this study. Singh (1996) contradicts Bailey's model and has theoretically shown that, for hydrated 1:1 layers, rolling is a preferable mechanism in comparison to tetrahedral rotation, and that kaolinite layers will roll once hydrated. The TEM data presented here provide unequivocal evidence in support of the new model put forward by Singh (1996).

Kaolinite and halloysite have similar chemical compositions in the 1:1 layer. Why one type of kaolin would form in preference to the other has been puzzling. The generally accepted view, based on the geographical occurrence of these 2 minerals, is that kaolinite crystallizes below a water table over long periods of time while halloysite forms in environments that promote rapid growth and disorder (Giese 1988). The findings of this study and the model presented by Singh (1996) provide a theoretical basis to explain these observations. In environments of high ionic concentration and rapid growth, such as near-surface weathering of volcanic ash, the 1:1 layers crystallize with abundant stacking disorder, which allows the retention of interlayer water. Since hydrated 1:1 layers prefer to correct lateral misfit of the tetrahedral and octahedral sheets by rolling instead of tetrahedral rotation (Singh 1996), a tubular or spheroidal halloysite forms directly from solution. However, in well-drained subsurface environments, a low ionic strength promotes slow growth with relatively less stacking disorder, and, consequently, non-hydrated planar kaolin, wherein lateral misfit is corrected by tetrahedral rotation, forms.

ACKNOWLEDGMENTS

We thank M. Quimio and A. Yago for laboratory assistance, D. Page for particle size analysis and R. Gould for the preparation of ultrathin sections. We are also grateful to J. B. Dixon and an anonymous reviewer for providing helpful comments.

REFERENCES

Bailey SW. 1989. Halloysite—A critical assessment. In: Farmer VC, Tardy Y, editors. Proceedings of the International Clay Conference; Strasbourg, France. Sci Geol Mem 86:89–98.

Bates TF, Hildebrand FA, Swineford A. 1950. Morphology and structure of endellite and halloysite. Am Mineral 6: 237–248.

Churchman GJ, Aldridge LP, Carr RM. 1972. The relationship between the hydrated and dehydrated states of an halloysite. Clays Clay Miner 20:241–246.

Costanzo PM, Clemency CV, Giese RF, Jr. 1980. Low temperature synthesis of a 10-Å hydrate of kaolinite using dimethylsulfoxide and ammonium fluoride. Clays Clay Miner 28:155–156.

Costanzo PM, Giese RF, Jr. 1985. Dehydration of synthetic hydrated kaolinites: a model for the dehydration of halloysite (10 Å). Clays Clay Miner 33:425–423.

Costanzo PM, Giese RF, Jr, Clemency CV. 1984. Synthesis of a 10-Å hydrated kaolinite. Clays Clay Miner 32:29–35.

Deed CT, van Olphen H, Bradley WH. 1966. Intercalation and interlayer hydration of minerals of the kaolinite group. In: Heller L, Weiss A, editors. Proceedings of the International Clay Conference; 1966; Jerusalem, Israel; Vol. 1. Jerusalem: Programs of Science in Translation. p 183–199.

Dixon JB, McKee TR. 1974. Internal and external morphology of tubular and spheroidal halloysite particles. Clays Clay Miner 22:127–137.

Giese RF, Jr. 1988. Kaolin minerals: structures and stabilities. Chapter 3. In: Bailey SW, editor. Hydrous phyllosilicates (exclusive of micas). MSA Rev Mineral 19:29–66.

Honjo G, Kitamura N, Mihama K. 1954. A study of clay minerals by means of single crystal electron diffraction diagrams—the structure of tubular kaolin. Clay Miner Bull 4:133–141.

Kohyama N, Fukushima K, Fukami A. 1978. Observation of the hydrated form of tubular halloysite by an electron microscope equipped with an environmental cell. Clays Clay Miner 26:25–40.

Mackinnon IDR, Uwins PJR, Yago AJE. 1993. Kaolinite particle sizes in the <2 μm range using laser scattering. Clays Clay Miner 41:613–623.

Radoslovich EW. 1963. The cell dimensions and symmetry of layer-lattice silicate: VI. Serpentine and kaolin morphology. Am Mineral 48:368–378.

Robertson IDM, Eggleton RA. 1991. Weathering of granitic muscovite to kaolinite and halloysite and of plagioclase-derived kaolinite to halloysite. Clays Clay Miner 39:113–126.

Singh B. 1996. Why does halloysite roll?—A new model. Clays Clay Miner 44:191–196.

Singh B, Gilkes RJ. 1992. An electron-optical investigation of the alteration of kaolinite to halloysite. Clays Clay Miner 40:212–229.

Uwins PJR, Mackinnon IDR, Thompson JG, Yago AJE. 1993. Kaolinite: NMF intercalates. Clays Clay Miner 41: 707–717.

Wada K. 1961. Lattice expansion of kaolin minerals by treatment with potassium acetate. Am Mineral 46:78–91.

Wada K. 1965. Intercalation of water in kaolin minerals. Am Mineral 50:924–941.

Wolfe RW, Giese RF, Jr. 1978. The stability of fluorine analogues of kaolinite. Clays Clay Miner 26:76–78.

(Received 17 July 1995; accepted 29 February 1996; Ms. 2670)